Int. J. Nano Dimens. 2026; 17(2) : 238-246

International Journal of Nano Dimension (IJND)

https://doi.org/10.57647/ijnd-2026-1702-08

Original Research

Band Gap Enhancement and Violet Luminescence from Chemically Synthesized Copper Oxide Nanospindles and Its Antimicrobial Activity Against *S. Aureus* and *K. Pneumoniae*

Suvayan Mandal[1,2], Pinaki Chakraborty[2], Pijus Kanti Samanta[3,*]

[1]*Department of Physics, Midnapore College (Autonomous), Paschim Medinipur, West Bengal, India*
[2]*Department of Physics, Raiganj University, Uttar Dinajpur, West Bengal, India*
[3]*Department of Physics, Prabhat Kumar College, Contai, Purba Medinipur, West Bengal, India*

[*]**Corresponding author:** pijush.samanta@gmail.com

Article History

Received:
9 August 2025
Revised:
9 September 2025
Accepted:
16 September 2025
Published online:
12 October 2025
Published in Issue:
10 April 2026

Abstract:

A simple wet-chemical method has been deployed to synthesize copper oxide (CuO) nanostructures. FESEM images revealed the formation of uniform-sized, spindle-like nanostructures. The TEM image revealed that the nanospindles are composed of several small crystallites. The distinct diffraction peaks in the XRD pattern confirm well-crystalline nanostructures and the average crystallite size was ~ 10 nm. FTIR spectra revealed the formation of Cu-O bonds. The band gap of the nanocrystals was calculated from the absorption spectra and was estimated to be 3.28 eV. Quantum confinement effect is therefore found to be very significant in these nanocrystals, manifested by the band gap enhancement. The synthesized CuO nanospindles exhibit strong photoluminescence peaked at ~ 407 nm owing to band-to-band transition. This emission peak is due to the transition associated with low energy peaks at ~ 461 nm due to shallow levels created below the bottom of the conduction band. The nanostructure showed significant antimicrobial activity against *S. Aureus* (Gram-positive) and *K. Pneumoniae* (Gram-negative) bacteria as studied by agar well diffusion technique. The zone of inhibition depends on the concentration of nanoparticles as revealed from the study. Therefore, the synthesized CuO is of immense potential for optoelectronics and biomedical applications.

Keywords: Antimicrobial; Band-gap; Crystallite; Nanospindles; Quantum-confinement

Cite this article: Mandal S, Chakraborty P, Kanti Samanta P. Afkhami A. Band Gap Enhancement and Violet Luminescence from Chemically Synthesized Copper Oxide Nanospindles and Its Antimicrobial Activity Against *S. Aureus* and *K. Pneumoniae*. Int. J. Nano Dimens. 2026;17(2): 238-246. https://doi.org/10.57647/j.ijnd.2026.1702.08

1. Introduction

Nanomaterials are of immense importance because of two phenomena- (i) high surface-to-volume ratio and (ii) quantum confinement. Large surface area compared to the same volume of bulk material results in more surface atoms that can be utilized for various catalytic and sensing applications. Again, due to small size, the carriers are confined within the narrow potential well of the crystal, resulting in the band gap enhancement in semiconductors and surface plasmon resonance in metallic nanoparticles. These properties are very useful in designing various optoelectronic and nanoelectronic devices, light emitting diodes, lasers, photodetectors; nanoparticles based drug delivery, and plasmonic therapy [1, 2, 3, 4, 5, 6, 7, 8, 9]. Several metals (Au, Ag, Cu) and semiconductor nanomaterials (Si, Ge, GaAs, InP) and their compounds (CuO, ZnO, TiO_2, CdS, ZnS, CdSe, PbS, CdTe) are at the forefront of materials research [10, 11, 12, 13, 14, 15, 16, 17]. Semiconducting metal oxides are very popular because of their unique optical and electrical properties, suitable for various optoelectronic and nanoelectronic applications. Amongst

the various compound semiconductors especially oxides, copper oxide (CuO) is of potential interest because of its excellent photocatalytic activity, carrier mobility in solar cells, and gas sensing applications [18, 19]. It is a direct and low band gap semiconductor with a band gap of ~ 1.8 eV [20]. However, the band gap can be tuned by tuning the particle size of CuO up to 3.2 eV [21]. It is a p-type semiconductor having potential application as an anode in lithium-ion batteries. It is also useful for the development of high-temperature superconductor composites and magnetoresistance [22, 23, 24, 25]. Furthermore, CuO exhibits photocatalytic properties also [26]. Researchers have synthesized CuO nanostructures of various morphologies such as nanorods, nanocages, nanocubes, nanoparticles, nanoflowers, and many more [27, 28, 29]. However, spindle-like CuO nanostructures are very rarely reported. One-step synthesis was used to create spindle-shaped CuO nanoparticles and their catalytic activity is reported by Ning et al. [30]. Harish and co-workers reported a solution-phase approach was to synthesize copper oxide nanospindles using high concentration of copper acetate and sodium hydroxide [31]. The spindles were porous in nature with size 70 nm × 150 nm. There are also reports synthesizing other hierarchical CuO nanostructures by the researchers. However, the detailed optical property of spindle-like CuO was not well investigated. It has been found in the literature that the morphology of the nanostructures plays an important role in optical, catalytic and antimicrobial activity [31, 32, 33, 34].

Al-Fa′ouri et. al. reported the chemical synthesis of CuO nanoparticles using leaves extract of Bougainvillea [35]. The reported band gap was very high (2.74 eV). The band gap was tuned to 3.34 eV by varying the PVA concentration. They also observed increased DC electrical conductivity with temperature. In another report, flower-like CuO nanostructures were synthesized in a hydrothermal process [36]. The size of the ultra-thin leaves of the nanoflowers was ~ 700 nm × 300 and the band gap was ~ 1.68 eV. The nanoflowers were reported to exhibit photocatalytic activities. Researchers have studied the antimicrobial activity of CuO against different bacteria such as *Escherichia coli*, *Pseudomonas aeruginosa*, *Enterococcus faecalis*, *Shigella flexneri*, *Salmonella typhimurium*, *Proteus vulgaris*. M. Ahamed et al. reported the antimicrobial activity of CuO nanoparticles [37]. They observed that the synthesized CuO nanoparticles were highly sensitive to *E. coli* and *E. faecalis* while less potent for *S. aureus*, *K. pneumonia*. Further, the studies on the antimicrobial activity against *S. aureus* and especially *K. pneumonia* are very limited [37].

To fill up this lacuna, in this paper, we report a simple chemical method to synthesize uniform-sized spindle-like CuO nanostructures, followed by typical structural and morphological characterization. Wet chemical method is very cost effective one and does not need the extreme parameters maintenance such as high temperature and low pressure as in various vapour deposition process. The spindle-like structure formation mechanism and morphological uniformity have also been discussed to understand the underlying bottom-up growth. The antimicrobial is necessary to understand the potent of the synthesized material as antimicrobial agent.

2. Experimental

All the chemicals used in this synthesis process were of analytical grade (99.99% pure) and used as supplied without further purification. In a typical synthesis process, 0.02 M $CuCl_2$ solution was prepared by dissolving 0.269 g of $CuCl_2$ in double-distilled water. 0.056 g of KOH was dissolved in distilled water to prepare a 1.0 M solution and kept under vigorous stirring. The $CuCl_2$ solution was then added drop-wise for 5 min, and the stirring was continued further for 2 h. A bluish precipitate was observed. At the end of the reaction, the precipitate was filtered and dried in an ordinary furnace at 110 °C for 2 h for further characterization. A schematic of the synthesis steps is shown in Fig. 1.

Morphology of the synthesized nanopowder was investigated in a ZEISS field-emission scanning electron microscope (FESEM) operating at 5 kV. For the FESEM imaging, the powder sample was first sprayed over a carbon tape and then gold-coated by thermal evaporation process. Crystallographic investigation was carried out by collecting the X-ray diffraction (XRD) data in Proto A-XRD X-ray diffractometer that uses a solid state detector to detect the diffracted X-ray. The source of X-rays was a Coolidge tube producing X-rays of wavelength 1.54 Å from a Cu target. The optical absorption spectra

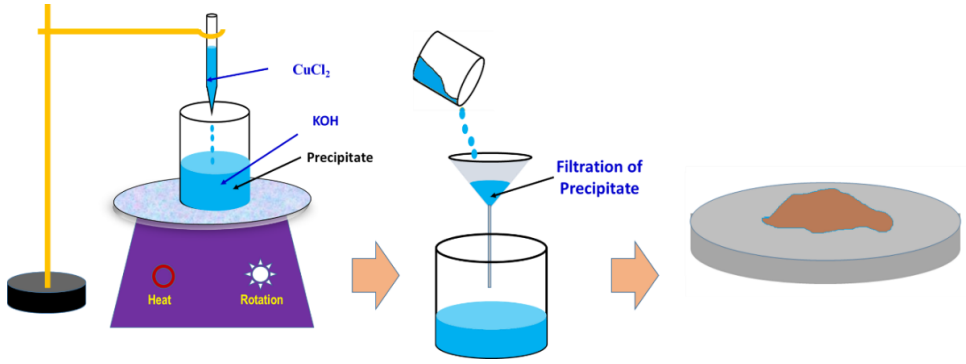

Figure 1. Schematic of the steps of synthesizing CuO nanostructure.

https://dx.doi.org/10.57647/j.ijnd.2026.1702.08

were recorded in a Perkin Elmer UV-Visible spectrophotometer in the wavelength range of 200 – 800 nm. Room temperature photoluminescence (PL) was investigated in a Perkin Elmer Spectrophotometer that uses a Xenon lamp as the source of excitation.

The Zone Inhibition Method (also known as the Kirby-Bauer method) was used to assess the antibacterial activity. The MHA plates were inoculated by spreading 100 µL of bacterial culture (the inoculum was made by adjusting the cell density by 0.5 McFarland Units, or 1.5 X 108 CFU/mL from Mueller-Hillinton Broth), and then the discs with 10 µL of varying concentration (0 to 100 mM) were placed on top of the plates. Ciprofloxacin discs (10 µg) were used as positive controls (PC), and one disc in each plate was filled with solvent only as a vehicle control. For twenty-four hours, the *S. Aureus* and *K. Pneumoniae* plates were incubated at 37 °C. The disc's surrounding clean zone was measured and noted.

3. Results and discussions

The morphology of the synthesized CuO was observed in FESEM. Typical FESEM images of the synthesized CuO nanostructures in different magnification are shown in Fig. 2. Spindle-like nanostructures are found to form in the chemical growth process. The spindles have uniform size distribution with dimensions: Length ~ 200 nm and breadth ~ 100 nm. It is also evident for the TEM image (Fig. 3). This spindle-like CuO nanostructure is not commonly observed and only few reports are found in the literature [31]. The underlying chemical reactions involved in the growth process are:

$$Cu^{2+} + 2OH^- \rightarrow Cu(OH)_2 \quad (1)$$

$$Cu(OH)_2 + 2OH^- \rightarrow [Cu(OH)_4]^{2-} \quad (2)$$

$$[Cu(OH)_4]^{2-} \rightarrow CuO + 2OH^- + H_2O \quad (3)$$

In the very initial stage, copper ions (Cu^{2+}) are formed due to dissolution of the copper salt in water. These copper ions, combining with the OH^- ions of water, produce $Cu(OH)_2$ nuclides by oxolation process. Hydrogen bonds of $Cu(OH)_2$, being very weak, are readily broken and react with OH^- ions to produce an ionic complex $[Cu(OH)_4]^{2-}$. Further decomposition of $[Cu(OH)_4]^{2-}$ nuclides results in the formation of CuO seeds. These CuO seeds grow further, and assembled together to form large-sized spindle-like nanocrystals. Further, it can be seen that the nanospindles are of uniform size, indicating the occurrence of diffusion diffusion-limited homonucleation process during chemical growth. A schematic of the growth mechanism is shown in Fig. 4.

Typical XRD pattern of the synthesized CuO nanospindles is shown in Fig. 5. Diffraction peaks were observed at 35.42°, 38.65°, 48.77°, and 58.13° corresponding to (110), (022), ($\bar{2}$02), and (202) planes of monoclinic unit cell of CuO, consistent with the JCPDS file no. 48-1548. The peaks are very sharp, indicating the formation of good-quality crystals. No impurity peaks were detected, which is a signature of the purity of the synthesized material. Crystallite size was calculated from the XRD pattern using the Scherrer equation [38]:

$$D = \frac{0.89\lambda}{\beta \cos\theta} \quad (4)$$

Here, β is the full-width at half-maxima of the diffraction peak appearing at Bragg angle (2θ) and λ is the wavelength of the X-ray used in the diffraction process. For this calculation, the highest intensity diffraction peak (110) peak and fitted with Lorentzian distribution function (see inset of Fig. 5). The crystallite size was calculated to be 10.4 nm. The crystallite size was found to be much less than the spindle-like nanostructures, indicating the formation of nanospindles by several grains. Therefore, the synthesized nanospindles are polycrystalline.

Typical FTIR spectrum of the synthesized CuO nanospindles is shown in Fig. 6. Various bands are observed. The band appearing at 521 cm^{-1}, 606 cm^{-1} and 1001 cm^{-1} are the characteristic features of CuO and corresponds to various stretching and bending modes of Cu-O bonds [39]. The band at 1599 cm^{-1} is due to the stretching modes of vibration of Cu-O. The bands appearing in the higher wave number (3160 cm^{-1} and 3442 cm^{-1}), is due to the stretching vibrational modes of water arising due to moisture absorption by the sample [40].

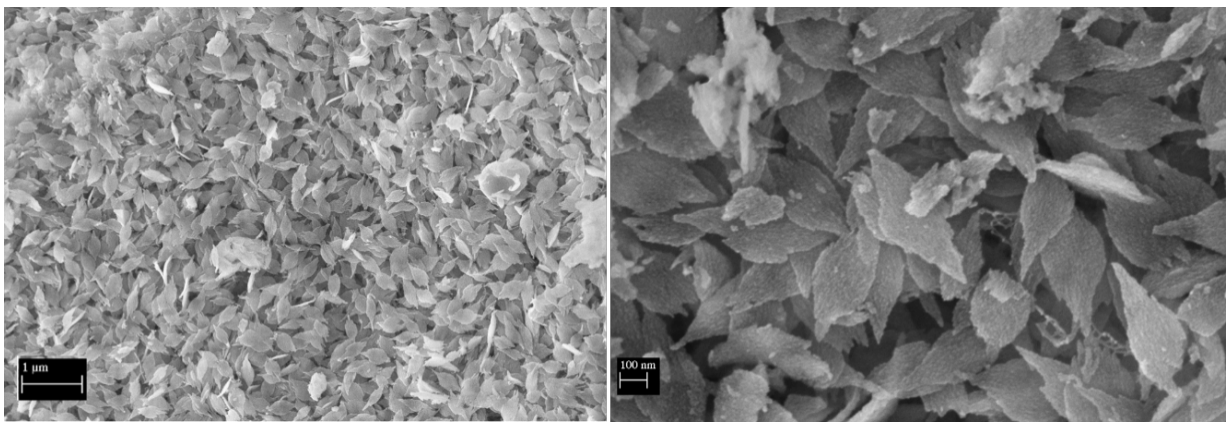

Figure 2. FESEM image of the synthesized CuO nanospindles in different magnifications.

https://dx.doi.org/10.57647/j.ijnd.2026.1702.08

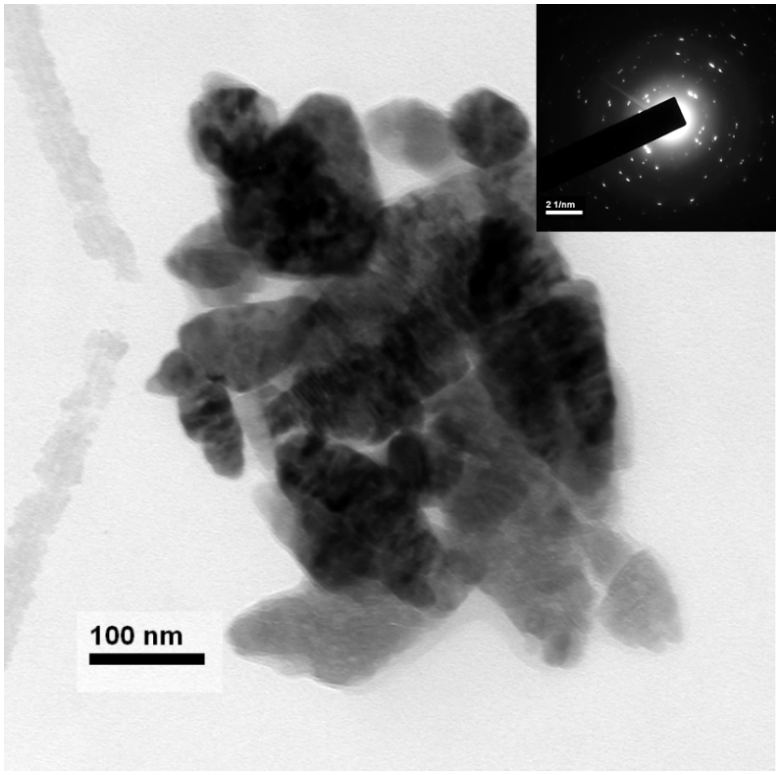

Figure 3. TEM image of the synthesized CuO nanospindles. Inset shows the selected area electron diffraction pattern indicating the crystalline nature of the material.

The light absorption property of the synthesized CuO nanospindles was studied using UV-visible absorption spectra as shown in Fig. 7 (a). It was observed that the absorption continuously decreases from UV to the visible region and has very low absorbance in the visible region. Therefore, this material can be used as transparent coatings in solar cells in visible region. The band gap (E_g) was calculated from the UV-visible absorption data using the Tauc equation [41]:

$$(\alpha h\nu)^n = C(h\nu - E_g) \tag{5}$$

Here, $h\nu$ is the incident photon energy, α is the material absorption coefficient, and C is a material constant. The value of the exponent n is 2 and 1/2, respectively, for direct and indirect band gap semiconductors. In the plot of $(\alpha h\nu)^2$ against $h\nu$ (Tauc plot) (see Fig. 7 (b)), drawing a tangent in the high absorption region, and taking the intercept with $(\alpha h\nu)^2 = 0$ axis, the band gap of the materials can be estimated. The band gap of synthesized CuO nanospindles was calculated to be 3.28 eV. Such high-band-gap CuO nanostructures are rarely reported [42]. Dagher et al. had also reported the high band gap CuO nanostructures with band gap of 3.25 eV [21]. the crystallite size was in the range of 5 – 10 nm. In our case, we also find the crystallite size ~ 10.4 nm which matches well with that reported in [42]. The band gap enhancement is mostly due to strong quantum confinement owing to small crystallite size.

Room temperature PL spectra of the synthesized CuO nanospindles, is shown in Fig. 8 (a). A broad PL spectrum was observed from UV to the visible region. The spectrum was deconvoluted, and two emission peaks at 407 nm (3.04) and 461 nm (2.69) were separated out. The emission peak at 407 nm has energy very close to

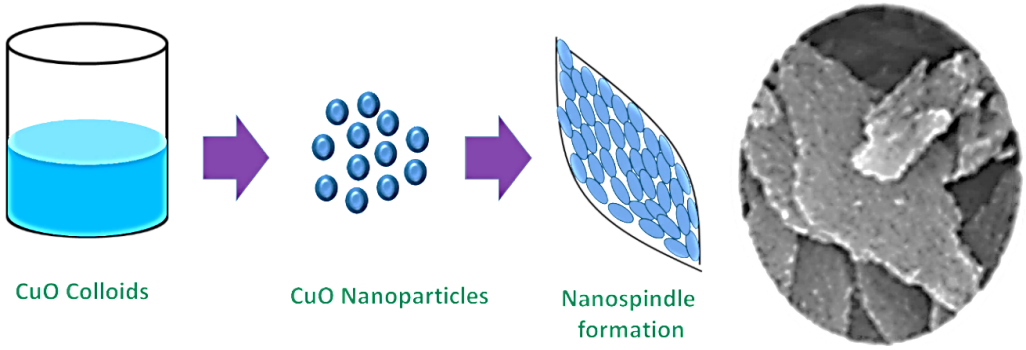

Figure 4. Schematic of the growth of the CuO nanospindles.

https://dx.doi.org/10.57647/j.ijnd.2026.1702.08

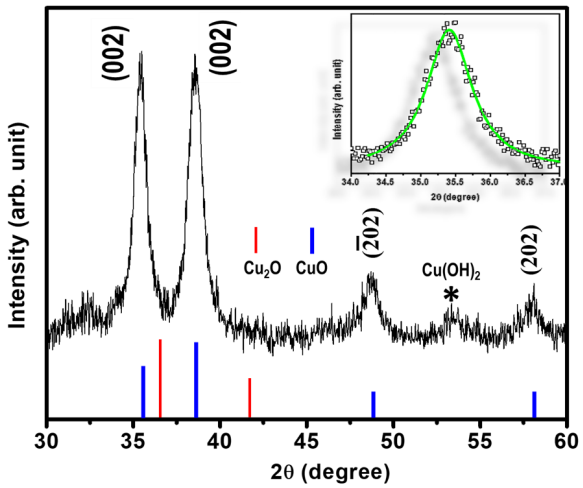

Figure 5. XRD pattern of the CuO nanospindles. The inset shows the fitting of the (110) peak for the estimation of the crystallite size.

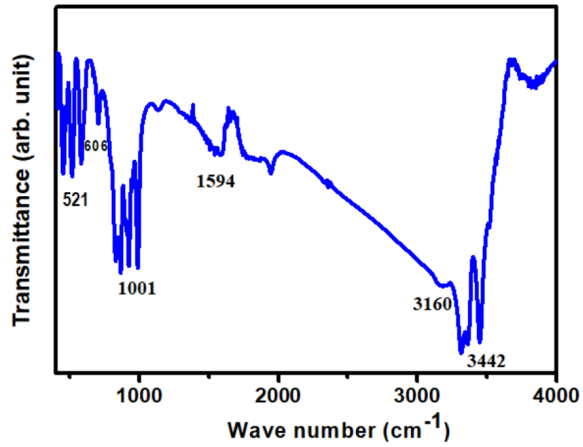

Figure 6. FTIR spectrum of the CuO nanospindles.

the band gap of the synthesized CuO nanostructures. Therefore, it can be associated with the direct band edge transition. In nanostructures, grown at low temperature wet-chemical synthesis, various defect states such as Cu vacancies and O- vacancies developed. These defect states produce shallow levels below the conduction band. When the nanostructures are excited by photons of energy larger than the band gap the electrons first excited to the conduction band. Some electrons may transit to the sub-band below the conduction band (see Fig. 8 (b)) by two processes- (i) carrier relaxation to shallow level donor states near the conduction band by non-radiative transition and radiative transition thereafter, or (b) radiatively jumps to shallow acceptor levels and relax thereafter to the valence band by thermalization [21]. Further, the PL spectrum is very broad which is the result of interaction of CuO nanoparticles with the ions of the solution and polydispersive particles [21].

The antimicrobial potent of the synthesized CuO nanospindles was investigated by studying the zone of inhibition in the agar plate. The variation of zone of inhibition with the nanoparticle concentration is also shown in Fig. 9 and Fig. 10. A dose-dependent antimicrobial activity against *S. Aureus* and *K. Pneumoniae* on agar plates revealed that, first visible at 50 µM and gradually increases with increasing concentration up to 1000 µM in our study. The antimicrobial activity of the synthesized CuO nanostructures against two clinically relevant *S. aureus* (Gram-positive) and *K. pneumoniae* (Gram-negative) bacteria have been used the conventional disc diffusion assay. Ciprofloxacin antibiotic was used as the positive control (PC) in this test. For both the bacteria, the zone of inhibition gradually increases with increased nanoparticle concentration. For *K. pneumoniae*, the results showed a definite concentration-dependent suppression. At 0 µM, no inhibition was seen, but at 50 µM, a little zone developed that gradually grew with increasing concentrations. At 1000 µM, the highest zone diameter was roughly 15 mm, while ciprofloxacin showed a substantially bigger zone (~ 32 mm). Between 250 and 500 µM, there was the most noticeable rise in activity; beyond that, the impact plateaued, suggesting that either the compound's antimicrobial efficacy was saturated or that its diffusion through the agar matrix was limited. Despite being much less effective than ciprofloxacin, these results demonstrate that the molecule has intrinsic activity against *K. pneumoniae*.

Likewise, for *S. aureus*, zone size increased gradually

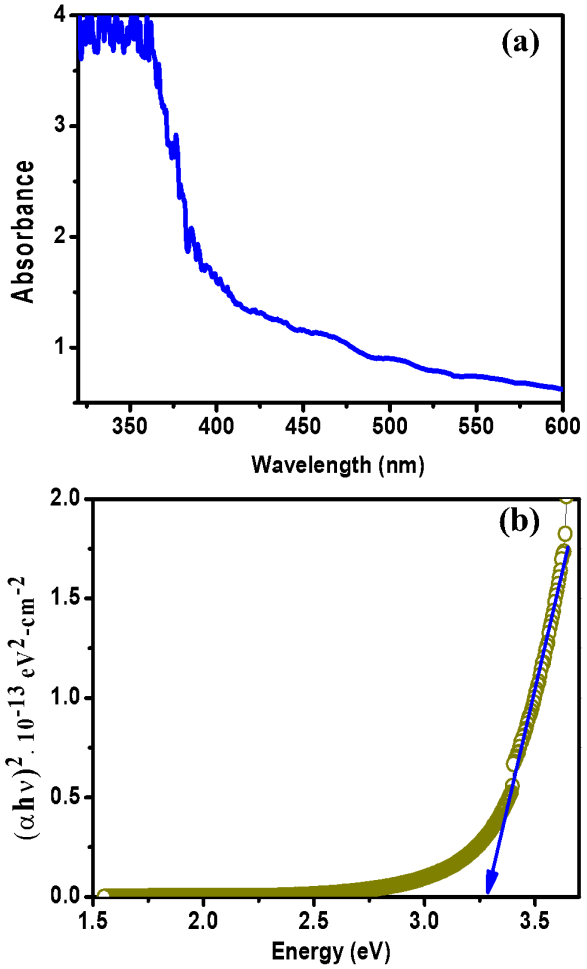

Figure 7. (a) UV-visible absorption spectra of the synthesized CuO nanospindles, (b) Tauc plot to calculate the band gap.

https://dx.doi.org/10.57647/j.ijnd.2026.1702.08

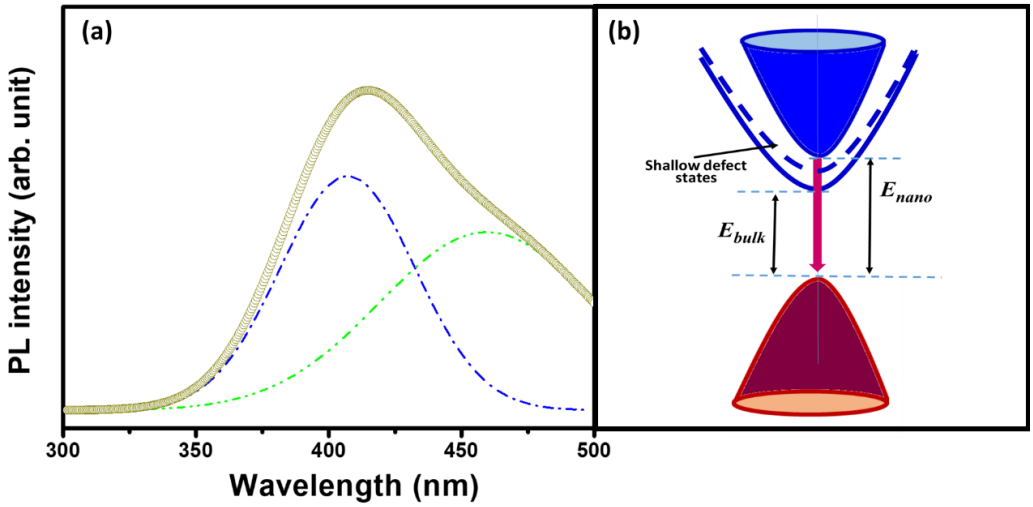

Figure 8. (a) Room temperature PL spectrum of the CuO nanospindles, (b) Schematic of energy bands showing the energy levels associated with the emitted photons.

as compound concentration increased. At 50 µM, the first notable inhibition was observed, and at 1000 µM, the maximal zone was ~ 10 mm, which was still far smaller than that of ciprofloxacin (~ 31 mm). There may have been a difference in the potent of the nanoparticles

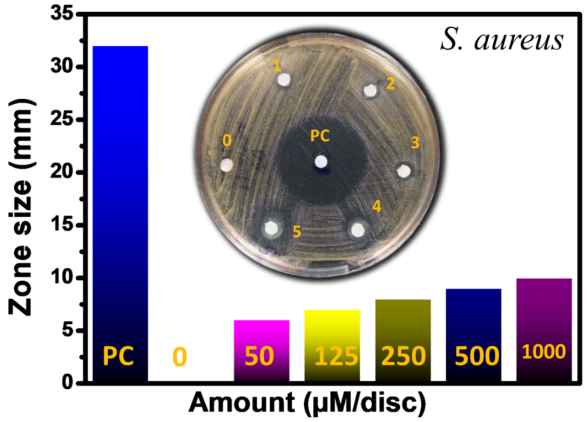

Figure 9. Diose dependent zone of inhibition of CuO nanospindles against *S. aureus*. Inset shows the inhibited disc.

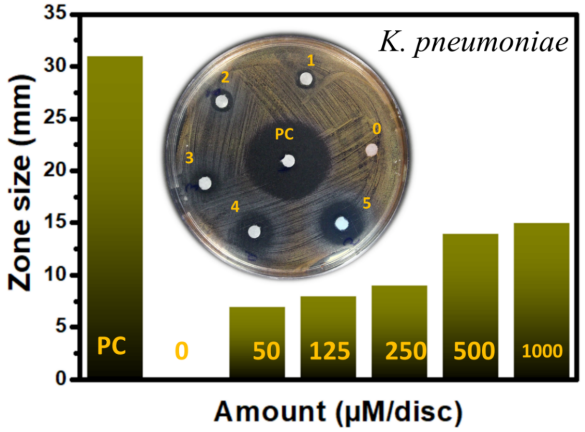

Figure 10. Diose dependent zone of inhibition of CuO nanospindles against *K. pneumoniae*. Inset shows the inhibited disc.

to interact with the bacterial cell wall or break through the thick peptidoglycan layer that is typical of Gram-positive bacteria, as the overall inhibitory effect against *S. aureus* was less than that reported for *K. pneumoniae*. These results are in line with earlier studies that showed that some new drugs were more effective against Gram-negative organisms because of variations in their efflux processes and outer membrane permeability [43, 44, 45]. The compound was marginally more effective against *K. pneumoniae* than *S. aureus*, according to a comparative analysis of the two organisms. This discrepancy could be caused by differences in target site accessibility, cell wall structure, and the compound's physicochemical characteristics that affect its activity and diffusion [46, 47, 48]. For both species, the plateauing effect observed at higher concentrations points to a restriction in the intrinsic bacteriostatic ability or solubility of CuO nanostructure.

4. Conclusion

In conclusion, we have successfully synthesized spindle-like CuO nanostructures by surfactant-free chemical method. The spindles are composed of several crystallites as observed from TEM image. The synthesized material is highly crystalline, as revealed from the XRD data. The formation fo various bonds were confirmed from FTIR spectra. The calculated band gap from the absorption data is very high which has an indication of strong quantum confinement effect. The synthesized CuO nanospindles exhibit visible photoluminescence which is remarkable. The visible photoluminescence resulted due to direct band edge transition and associated defect related shallow level transitions. Furthermore, the CuO nanospindles are found to be antimicrobial against *S. Aureus* and *K. Pneumoniae*. Therefore, the synthesized CuO nanospindles will have potential applications in optoelectronics and as well as in biomedical research.

https://dx.doi.org/10.57647/j.ijnd.2026.1702.08

Acknowledgement
The authors sincerely acknowledge UGC-DAE-CSR Kalpakkam node for FESEM facility and UGC-DAE-CSR Kolkata centre for providing UV-visible and Photoluminescence spectroscopy characterization facilities to carry out this research work. The author SM also sincerely acknowledges Midnapore College (autonomous) for necessary support. The author PKS sincerely acknowledge DST-FIST, PKC for various facilities for execution of the work.

Authors contributions
All authors contributed equally to the conception, design, execution, and writing of this work. All authors read and approved the final manuscript.

Availability of data and materials
The authors declare that the data supporting the findings of this study are available within the paper.

Conflict of interests
The authors assert that they do not have any identifiable conflicting financial interests or personal relationships that might be perceived to influence the work presented in this paper.

References

1. Barhoum A, García-Betancourt ML, Jeevanandam J, Hussien EA, Mekkawy SA, Mostafa M, Omran MM, Abdalla MS, and Bechelany M. "Review on Natural, Incidental, Bioinspired, and Engineered Nanomaterials: History, Definitions, Classifications, Synthesis, Properties, Market, Toxicities, Risks, and Regulations. " Nanomaterials 2022; 12:177. DOI: 10.3390/nano12020177
2. Abdel-Amir H and Habeeb MA. "Fast and Simple Fabrication of ternary PVA/CeO_2/SiC Nanocomposites for Optoelectronic and Antimicrobial Applications. " Silicon 2024; 16:2703. DOI: 10.1007/s12633-024-02874-4
3. Samanta PK. "Optical Properties of Hydrothermally Grown ZnO Nanoflowers. " Nanoscience & Nanotechnology-Asia 2022; 12:39. DOI: 10.2174/2210681212666220513095658
4. Habeeb MA and Mahdi S. "Influence of ZrC nanofiler on the structural, dielectric and optical features of the PVA–PVP blend for electronic and optical nanodevices. " Opt Quant Electron. 2023; 55:1076. DOI: 10.1007/s11082-023-05426-z
5. Samanta PK. "Effect of microstrain on the crystallite size of ZnO nanoparticles: X-ray peak profile and Rietveld analysis." Next Materials 2025; 8:100841. DOI: 10.1016/j.nxmate.2025.100841
6. Hamza RSA and Habeeb MA. "Reinforcement of morphological, structural, optical, and antibacterial characteristics of PVA/CMC bioblend filled with SiO_2/Cr_2O_3 hybrid nanoparticles for optical nanodevices and food packing industries." Polym. Bull. 2024; 81:4427. DOI: 10.1007/s00289-023-04913-3
7. Taha A, AL-Jawad SMH, and Redha AM. "Preparation and characterization of nanostructure CuS for biological activity. " J. Am. Chem. Soc. 2019; 33:1950374. DOI: 10.1142/S0217984919503743
8. Samanta PK. "Band Gap Engineering, Quantum Confinement, Defect Mediated Broadband Visible Photoluminescence and Associated Quantum States of Size Tuned Zinc Oxide Nanostructures." Optik-IJLEO. 2020; 221:165337. DOI: 10.1016/j.ijleo.2020.165337
9. Al-Jawad SMH, Taha AA, Redha AM, and Imran NJ. "Influence of nickel doping concentration on the characteristics of nanostructure cus prepared by hydrothermal method for antibacterial activity. " Surface Review and Letters 2021; 28:2050031. DOI: 10.1142/S0218625X20500316
10. Yang Z and Shen J. "Non-adiabatic excited state dynamics in atomically precise gold nanoclusters: the role of ligand networking interactions." Nanoscale 2025; 7:15068. DOI: 10.1039/D5NA00358J
11. More P, Inamdar V, Suresh S, Dindorkar S, Peddakolmi S, Jain K, Khona N, Khatoon S, and Patange S. "Synthesis of zinc oxide nanoparticles using *Chrysopogonzizanioides* grass extract, its applications in photodegradation and antimicrobial activity. " J. Mater. Sci: Mater. Electron. 2021; 32:20725. DOI: 10.1007/s10854-021-06585-z
12. Barman K, Chakraborty P, and Samanta PK. "Green Synthesis of Zinc Oxide Nanostructure using Azadirachta Indica Leaf Extract and its Structural and Microstructural Study." Physica Scripta 2021; 96:035704. DOI: 10.1088/1402-4896/abda6c
13. Ansari Z, Kadam S, Kasabe S, Tripathi J, Agale P, Patange S, and More P. "Optimized Mn doped ZnO@rGO nanocomposites: a breakthrough for advanced energy storage and PEC systems." Ionics 2025; 31:8151. DOI: 10.1007/s11581-025-06468-x
14. Ning Y, Guan Y, Zhang N, Song W, Zhang F, Chen L, and Chai F. "Exploring the Spindle-Shaped Copper Oxide Nanoparticles as Cost-Effective Catalyst. " Chemistry Select 2022; 7:e202200626. DOI: 10.1002/slct.202200626
15. Harish S, Navaneethan M, Archana J, Ponnusamy S, Muthamizhchelvan C, and Hayakawa Y. "Chemical synthesis and properties of spindle-like CuO nanostructures with porous nature. " Materials Letters 2015; 139:59. DOI: 10.1016/j.matlet.2014.10.002
16. Abideen ZU, Bibi S, and Liu H. "Designing Robust CdS Nanostructures for Superior Photostability and Enhanced Photocatalytic Degradation of Organic Pollutants. " Chemistry Select 2024; 9:e202401951. DOI: 10.1002/slct.202401951

17. Haghighi FH, Mercurio M, Cerra S, Salamone TA, C. Palocci RB andd, Spicac VR, and Fratoddi I. "Surface modification of TiO_2 nanoparticles with organic molecules and their biological applications. " 2023; J. Mater. Chem. B:2334. DOI: 10.1039/D2TB02576K
18. Khodadad H, Hatamjafari F, Pourshamsian K, and Sadeghi B. "Microwave-assisted Synthesis of Novel Pyrazole Derivatives and their Biological Evaluation as Anti-Bacterial Agents. " Combinatorial Chemistry & High Throughput Screening 2021; 24:695. DOI: 10.2174/1386207323666201019152206
19. Chowdhury MM and Samanta PK. Green Luminescent CdS Quantum Dots: Synthesis, Characterization and Antifungal Activity against Aspergillus niger. 2025. DOI: 10.26434/chemrxiv-2025-02xgl
20. Verma N and Kumar N. "Cerebral Organoid-on-a-Chip: A 3D Microfluidic Culture Model with Flow-Induced Shear Stress." ACS Biomaterials Science & Engineering 2019; 5:1170. DOI: 10.1021/acsbiomaterials.8b01633S
21. Dagher S, Haik Y, Ayesh AI, and Tit N. "Synthesis and optical properties of colloidal CuO nanoparticles. " J. Luminescence 2014; 151:149. DOI: 10.1016/j.jlumin.2014.02.015
22. Pourjafari M, Ghane M, Kaboosi H, Sadeghi B, and Rezaei A. "Antibacterial Properties of Ag–Cu Alloy Nanoparticles Against Multidrug-Resistant Pseudomonas aeruginosa Through Inhibition of Quorum Sensing Pathway and Virulence-Related Genes." J. Biomed. Nanotechnol 2022; 18:1196. DOI: 10.1166/jbn.2022.3331
23. Azari B, Pourahmad A, Sadeghi B, and Mokhtary M. "Green synthesis of SiO_2 from Equisetnm arvense plant for synthesis of SiO_2/ZIF-8 MOF nanocomposite as photocatalyst." J. Coord. Chem. 2023; 76:219. DOI: 10.1080/00958972.2023.2166408
24. Samanta PK and Kamilya T. "Optical Properties of Surface Modified ZnO Nanorods. " J. Nanoeng. Nanomanufac. 2014; 4:173. DOI: 10.1166/jnan.2014.1176
25. Akintelu SA, Folorunso AS, Folorunso FA, and Oyebamiji AK. "Green synthesis of copper oxide nanoparticles for biomedical applications." Heliyon 2020; 6:e04508. DOI: 10.1016/j.heliyon.2020.e04508
26. Fu S, Zheng Y, Zhou X, Ni Z, and Xia S. "Visible light promoted degradation of gaseous volatile organic compounds catalyzed by Au supported layered double hydroxides: Influencing factors, kinetics and mechanism. " J. Hazard. Mater. 2019; 363:41–54. DOI: 10.1016/j.jhazmat.2018.10.009
27. Ayoman E, Hossini G, and Haghighi N. "Synthesis and Characterization of Spherical Zinc Oxide Nanoparticles by a Simple Wet Chemical Method . " Int. J. Nanosci. Nanotechnol 2015; 11:63. DOI: 10.12781/ijsn.2015.11.1.0069
28. Nikam AV, Prasad BLV, and Kulkarni AA. "Wet chemical synthesis of metal oxide nanoparticles: a review. " Cryst. Eng. Comm. 2018; 20:5091. DOI: 10.1039/C8CE00487K
29. Sadeghi B and Vahdati R. "Comparison and SEM-characterization of novel solvents of DNA/carbon nanotube. " Appl. Surf. Sci. 2012; 258:3086. DOI: 10.1016/j.apsusc.2011.11.042
30. Ning Y, Guan Y, Zhang N, Song W, Zhang F, Chen L, and Chai F. "Exploring the Spindle-Shaped Copper Oxide Nanoparticles as Cost-Effective Catalyst." Chemistry Select. 7
31. Harish S, Navaneethan M, Archana J, Ponnusamy S, Muthamizhchelvan C, and Hayakawa Y. "Chemical synthesis and properties of spindle-like CuO nanostructures with porous nature." Materials Letters 2015; 139:59. DOI: 10.1016/j.matlet.2014.10.002
32. More P, Jangam K, Kadam S, Balgude S, Ajagekar S, and Yamgar R. "Co_3O_4 supported on MWCNT: A highly efficient nano composite for the adsorption of Coracryl yellow dye and in the reduction of 4-Nitrophenol." Results in Chemistry 2023; 5:100963. DOI: 10.1016/j.rechem.2023.100963
33. Mekuye B and Abera B. "Nanomaterials: An overview of synthesis, classification, characterization, and applications. " Nano Select 2023; 4:486. DOI: 10.1002/nano.202300038
34. Agale P, Salve V, Mardikar S, Patange S, and More P. "Synthesis and characterization of hierarchical Sr-doped ZnO hexagonal nanodisks as an efficient photocatalyst for the degradation of methylene blue dye under sunlight irradiation." Appl. Surf. Sci. 2024; 672:160795. DOI: 10.1016/j.apsusc.2024.160795
35. Al-Fa′ouri AM, Abu-Kharma M, and Awwad A. "Green Synthesis of Copper Oxide Nanoparticles Using Bougainvillea Leaves Aqueous Extract and Antibacterial Activity Evaluation." Arabian Journal of Chemistry 2023; 16:104535. DOI: 10.5281/zenodo.4899095
36. Al-Fa′ouri M, Lafi OA, Abu-Safe HH, and Abu-Kharma M. "Investigation of optical and electrical properties of copper oxide - polyvinyl alcohol nanocomposites for solar cell applications." Arabian Journal of Chemistry 2023; 16:104535. DOI: 10.1016/j.arabjc.2022.104535
37. Ahamed M, Alhadlaq HA, Khan MAM, Karuppiah P, and Al-Dhabi NA. "Synthesis, Characterization, and Antimicrobial Activity of Copper Oxide Nanoparticles. " Journal of Nanomaterials 2014; 2014:637858. DOI: 10.1155/2014/637858

38. Sahu S and Samanta PK. "Microstructural study and crystallite size analysis of chemically grown bougainvillea flower-like zinc oxide nanostructures." Materials Today Proceedings 2022; 65:2502. DOI: 10.1016/j.matpr.2022.04.474

39. Matei A, Craciun G, Romanitan C, Pachiu C, and Tucureanu V. "Biosynthesis and Characterization of Copper Oxide Nanoparticles." Engineering Proceedings 2023; 37:54. DOI: 10.3390/ECP2023-14629

40. Nzilu DM, Madivoli ES, Makhanu DS, Wanakai SI, Kiprono GK, and Kareru PG. "Green synthesis of copper oxide nanoparticles and its efficiency in degradation of rifampicin antibiotic." Sci Rep 2023; 13:14030. DOI: 10.1038/s41598-023-41119-z

41. Bhattacharya P, Swarnakar S, Ghosh S, Majumdar S, Banerjee S, and Environ J. "Disinfection of drinking water via algae mediated green synthesized copper oxide nanoparticles and its toxicity evaluation. " Journal of Environmental Chemical Engineering 2019; 7:102867. DOI: 10.1016/j.jece.2018.102867

42. Mallick P and Sahu S. "Structure, Microstructure and Optical Absorption Analysis of CuO Nanoparticles Synthesized by Sol-Gel Route. " Nanoscience and Nanotechnology 2012; 2:71. DOI: 10.5923/j.nn.20120203.05

43. Bouafia A, Laouini SE, and Ouahrani MR. "A Review on Green Synthesis of CuO Nanoparticles using Plant Extract and Evaluation of Antimicrobial Activity. " Asian J Res Chem 2020; 13:65. DOI: 10.5958/0974-4150.2020.00014.0

44. Chen M, He Y, Ye Q, Zhang Z, and Y YH. "Experimental study on convective heat transfer of a novel helical coil heat exchanger with porous media. " Int J Heat Mass Transf 2019; 130:1133. DOI: 10.1016/j.ijheatmasstransfer.2018.10.111J

45. Zhang J, Wang H, Wang Q, Sun Z, Buhe B, Sun Y, and Meng C. "Facile fabrication of a spindle-like CuO anchored on Graphene nanocomposite with relative high-rate performance and cycle stability for flexible supercapacitor. " J Mater Sci: Mater Electron 2022; 33:11143. DOI: 10.1007/s10854-022-08182-4

46. Cao D, Shu X, Zhu D, Liang S, Hasan M, and Gong S. "Green synthesis of zinc oxide nanoparticles and their application in biomedical fields. " Nano Convergence 2020; 7:14. DOI: 10.1186/s40580-020-00226-6

47. Gupta SV, Kulkarni VV, and Ahmaruzzaman M. Sci Rep 2023; Biosynthesis of Silver Nanoparticles from Bauhinia variegata Linn. Leaf Extract and Their Antibacterial Activity against Multidrug-Resistant Clinical Pathogens.:3009. DOI: 10.1038/s41598-023-29472-3

48. Debart A, Dupont L, Poizot P, Leriche J, and Tarascon J. "A Transmission Electron Microscopy Study of the Reactivity Mechanism of Tailor-Made CuO Particles Toward Lithium. " J Electrochem Soc 2001; 148:A1266. DOI: 10.1149/1.1409971